Heteroatom Chemistry
Volume 17, Number 7, 2006

Steric Effects on the Dialkyl Substituted X_2C_2Si Silylenes: A Theoretical Study

M. Z. Kassaee, S. M. Musavi, S. Soleimani-Amiri, and M. Ghambarian

Department of Chemistry, Tarbiat Modarres University, P.O. Box 14115-4838, Tehran, Iran

Received 5 July 2005; revised 10 October 2005

ABSTRACT: *With the aim of recognizing the steric effects on the silylenic H_2C_2Si structures, ab initio and DFT calculations are carried out on 24 structures of X_2C_2Si (where X is hydrogen (H), methyl (Me), isopropyl (i-pro), and tert-butyl (tert-Bu)). These species are at either triplet (t) or singlet (s) states. They are confined to the following three sets of structures ($\mathbf{1}_X$, $\mathbf{2}_X$ and $\mathbf{3}_X$). Structures $\mathbf{1}_X$ include silacyclopropenylidenes ($\mathbf{1}_{\text{s-H}}$ and $\mathbf{1}_{\text{t-H}}$) and their 2,3-disubstituted derivatives ($\mathbf{1}_{\text{t-Me}}$, $\mathbf{1}_{\text{s-Me}}$; $\mathbf{1}_{\text{t-}i\text{-pro}}$, $\mathbf{1}_{\text{s-}i\text{-pro}}$; $\mathbf{1}_{\text{t-}tert\text{-Bu}}$, $\mathbf{1}_{\text{s-}tert\text{-Bu}}$). Structures $\mathbf{2}_X$ include vinylidenesilylenes ($\mathbf{2}_{\text{s-H}}$ and $\mathbf{2}_{\text{t-H}}$) and their 3,3-disubstituted derivatives ($\mathbf{2}_{\text{t-Me}}$, $\mathbf{2}_{\text{s-Me}}$; $\mathbf{2}_{\text{t-}i\text{-pro}}$, $\mathbf{2}_{\text{s-}i\text{-pro}}$; $\mathbf{2}_{\text{t-}tert\text{-Bu}}$, $\mathbf{2}_{\text{s-}tert\text{-Bu}}$). Structures $\mathbf{3}_X$ include ethynylsilylenes ($\mathbf{3}_{\text{s-H}}$ and $\mathbf{3}_{\text{t-H}}$) and their 1,3-disubstituted derivatives ($\mathbf{3}_{\text{t-Me}}$, $\mathbf{3}_{\text{s-Me}}$; $\mathbf{3}_{\text{t-}i\text{-pro}}$, $\mathbf{3}_{\text{s-}i\text{-pro}}$; $\mathbf{3}_{\text{t-}tert\text{-Bu}}$, $\mathbf{3}_{\text{s-}tert\text{-Bu}}$). Singlet–triplet energy separations ($\Delta E_{\text{s-t,X}}$) and relative energies for the above structures are acquired at HF/6-31G*, B_1LYP/6-31G*, B3LYP/6-31G*, MP2/6-31G*, HF/6-31G**, B1LYP/6-31G**, B3LYP/6-31G**, and MP2/6-31G** levels of theory. The highest $\Delta E_{\text{s-t,X}}$ is encountered for $\mathbf{1}_X$. All singlet states of X_2C_2Si, are more stable than their corresponding triplet states. Linear correlations are found between the LUMO–HOMO energy gaps of the singlet $\mathbf{1}_{s\text{-}X}$ and $\mathbf{2}_{s\text{-}X}$ with their corresponding singlet–triplet energy separations calculated at B3LYP/6-31G**. The seven structures $\mathbf{2}_{\text{s-Me}}$, $\mathbf{2}_{\text{t-Me}}$, $\mathbf{3}_{\text{s-Me}}$, $\mathbf{1}_{\text{t-Me}}$, $\mathbf{1}_{\text{s-Me}}$, $\mathbf{1}_{\text{s-}tert\text{-Bu}}$, and $\mathbf{3}_{\text{t-}tert\text{-Bu}}$ do not appear to be real isomers. Different stability orders are obtained as a function of the substituents (X). The order of stability for six isomers of H_2C_2Si is $\mathbf{1}_{\text{s-H}} > \mathbf{2}_{\text{s-H}} > \mathbf{3}_{\text{s-H}} > \mathbf{2}_{\text{t-H}} > \mathbf{3}_{\text{t-H}} > \mathbf{1}_{\text{t-H}}$. Replacing hydrogen atoms by methyl group (X = Me) presents a new stability order: $\mathbf{1}_{\text{s-Me}} > \mathbf{3}_{\text{s-Me}} > \mathbf{2}_{\text{s-Me}} > \mathbf{3}_{\text{t-Me}} > \mathbf{2}_{\text{t-Me}} > \mathbf{1}_{\text{t-Me}}$; and for (i-pro)$_2C_2Si$ is $\mathbf{1}_{\text{s-}i\text{-pro}} > \mathbf{2}_{\text{s-}i\text{-pro}} \approx \mathbf{3}_{\text{s-}i\text{-pro}} > \mathbf{3}_{\text{t-}i\text{-pro}} \approx \mathbf{2}_{\text{t-}i\text{-pro}} > \mathbf{1}_{\text{t-}i\text{-pro}}$. Using the larger tert-butyl group as a substituent (X), yet it offers a more different stability order for six structures of (tert-Bu)$_2C_2Si$: $\mathbf{1}_{\text{s-}tert\text{-Bu}} > \mathbf{3}_{\text{s-}tert\text{-Bu}} > \mathbf{2}_{\text{s-}tert\text{-Bu}} > \mathbf{3}_{\text{t-}tert\text{-Bu}} > \mathbf{1}_{\text{t-}tert\text{-Bu}} > \mathbf{2}_{\text{t-}tert\text{-Bu}}$. Among eight levels employed, B3LYP/6-31G** appears as the method of choice.* Heteroatom Chem 17:619–633, 2006; DOI 10.1002/hc.20204

INTRODUCTION

Recently much attention has been directed toward the chemistry of heavy carbene analogues [1–10]. Chemical species which involve divalent silicon atoms, silylenes, are key intermediates in numerous thermal and photochemical reactions of organosilicon compounds [4]. Besides, much interest has been focused on their bonding properties and reactivities such as addition to olefins [11,12], alkynes [13], isocyanides [14], and transition metal complexes [15] in connection with the reactivities of carbenes. The multiple-bond compounds including second period elements such as olefin, imine (Schiff base), ketone, acetylene, nitrile, etc. are stable compounds and play a very important role in organic chemistry. Contrary to this, multiple-bond compounds containing

---

Correspondence to: M. Z. Kassaee; e-mail: Drkassaee@yahoo.com, Kassaeem@modares.ac.ir

elements from the third period onward (named as heavier main group elements) have long bond distances, and their π-bond energy generated through the overlapping of p-orbitals is low so that they are extremely unstable [16–18]. Thus, it was more surprising that the first homo-nuclear bond was realized with tin in a distannene by Lappert et al. [19]. The first disilene was prepared in 1981 by West, because in analogy to the alkenes, its double bond was shortened in comparison to the Si—Si single bond length, and the transbending of the substituents was appreciably less pronounced than in the distannene [20]. Shortly later, Masamune *et al.* reported not only on the first examples of the cyclotrisilanes, cyclotrigermanes, and cyclotristannanes but also on their photochemical or thermal ring cleavages to afford disilenes, digermenes, and one, although not isolable, distannene [21–23]. These results appear to suggest that the chemistry of multiple bonds between the heavier elements of group 14 has been more or less completely unknown [24]. However, the recent successful isolation of a trisilaallene [25], together with the more well-known tristannaallene [26], shows that the potential for novel compounds is by no means exhausted.

Recently, among small silylenes with many interesting bonding and energetic characteristics, C_2H_2Si species has become the topic of a great number of theoretical as well as a small number of experimental reports [27,28]. We have already reported the results of ab initio studies on halogenated isomers of C_2H_2Si [3]. Though, up to date no attempt has been made to account for steric effects on C_2H_2Si derivatives. The present work scrutinizes the steric effects on the energy surface and stability of singlet (s) and triplet (t) X_2C_2Si silylenes $\mathbf{1}_X$–$\mathbf{3}_X$, where X is hydrogen, methyl, isopropyl, and *tert*-butyl (Fig. 1).

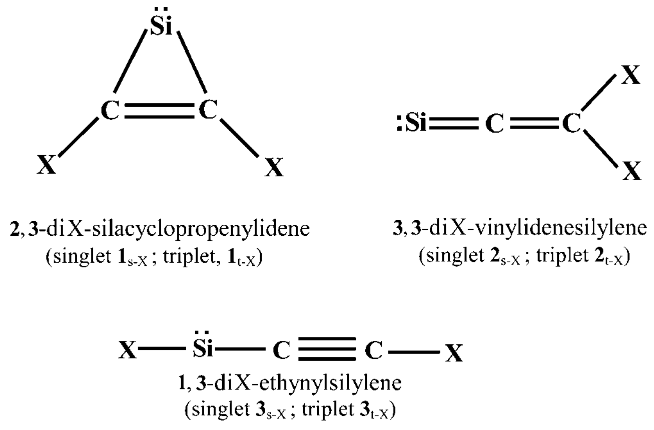

FIGURE 1 The three most significant structures considered for singlet (s) and triplet (t) silylenic X_2C_2Si (**1**, **2**, and **3**, where X is H, CH_3, $(CH_3)_2CH$, and $(CH_3)_3C$).

COMPUTATIONAL METHODS

Geometries of singlet and triplet H_2C_2Si silylenes, as well as their dialkyl-substituted analogues, $(CH_3)_2C_2Si$, $((CH_3)_2CH)_2C_2Si$, and $((CH_3)_3C)_2C_2Si$, confined to the three skeletal arrangements of 2,3-diX-silacyclopropenylidene ($\mathbf{1}_X$), 3,3-diX-vinylidenesilylene ($\mathbf{2}_X$) and 1,3-diX-ethynylsilylene ($\mathbf{3}_X$) are fully optimized at the HF, DFT, and MP2 methods, where X is H, Me, *i*-Pro, and *tert*-Bu (Fig. 1). For Hartree–Fock (HF) level of theory, 6-31G** and 6-31G** basis sets are used. For density functional theory (DFT) calculations, the Becke's hybrid one-parameter and three-parameter functional using the Lee–Yang–Parr correlation including both local and nonlocal terms as implemented by Adamo and Barone [29–31] with the 6-311G* and 6-31G** basis sets are employed. For the second-order Møller–Plesset (MP2) method [32] again the 6-311G* and 6-31G** basis sets are used. Singlet states are calculated with spin-restricted wave function. Triplet states are calculated using the UHF, UB1LYP, UB3LYP, and UMP2 formalisms. The energies of HOMO and LUMO orbitals are obtained through NBO analysis [33] for all 24 X_2C_2Si silylenes. The harmonic vibrational frequencies and zero-point energies (ZPE) are calculated for each HF and DFT optimized structures at the same level of theory. The vibrational frequencies and ZPE data at the HF and B3LYP are scaled by 0.89 and 0.98, respectively [34,35]. This is to account for the difference between the harmonic and anharmonic oscillations of the actual bonds. For minimum state structures, only real-frequency values (positive sign) and for the transition states, only a single imaginary frequency value (negative sign) is accepted. All calculations in this work are performed using the Gaussian 98 program package [36].

RESULTS AND DISCUSSION

We have deliberately included data from eight levels of theory, since reporting results of various levels may offer an opportunity to compare different levels. Energetic results are dependent on the computational methods employed but not much dependent on the basis sets applied. These differences are more pronounced for triplet species, may be due to the spin-contamination problem which is encountered for MP2 and/or HF calculations [37,38]. Nevertheless, a rather manifest consistency is found between the calculated relative energy trends (Tables 1–4). One may ask why in this work B3LYP/6-31G** is chosen over other calculation methods. The reliability of various density functional theory (DFT) methods has already been evaluated for the study

TABLE 1 Relative Energies, with ZPE Corrections, for Singlet $\mathbf{1}_{\text{s-H}}$, $\mathbf{2}_{\text{s-H}}$, and $\mathbf{3}_{\text{s-H}}$ as Well as Triplet States $\mathbf{1}_{\text{t-H}}$, $\mathbf{2}_{\text{t-H}}$, and $\mathbf{3}_{\text{t-H}}$ of Silylenic $(H)_2C_2Si$

	Relative Energies (kcal/mol)								*Dipole Moments (D)*	*Vibrational Zero Point Energies (kcal/mol)*
Structure	*HF/ 6-31G**	*HF/ 6-31G***	*B1LYP/ 6-31G**	*B1LYP/ 6-31G***	*B3LYP/ 6-31G**	*B3LYP/ 6-31G***	*MP2/ 6-31G**[a]	*MP2/ 6-31G***[a]	*B3LYP/ 6-31G***	*B3LYP/ 6-31G***
$\mathbf{1}_{\text{s-H}}$[b]	[1]0.00	[2]0.00	[3]0.00	[4]0.00	[5]0.00	[6]0.00	[7]0.00	[8]0.00	1.29	18.65
$\mathbf{1}_{\text{t-H}}$	60.52	60.51	71.06	70.86	71.06	71.07	70.51	59.58	0.94	17.07
$\mathbf{2}_{\text{s-H}}$	20.62	20.81	15.34	15.17	14.75	15.36	19.90	20.25	1.47	18.13
$\mathbf{2}_{\text{t-H}}$	24.61	25.83	88.52	35.54	36.03	36.99	50.49	50.73	1.70	18.21
$\mathbf{3}_{\text{s-H}}$	18.13	18.42	20.26	20.58	20.54	20.86	24.50	24.83	1.28	15.47
$\mathbf{3}_{\text{t-H}}$	24.76	24.94	43.92	44.06	44.40	44.54	50.62	51.30	0.55	15.42

Relative energies are calculated at six levels of theory, where global minimum is set at 0.00 kcal/mol along with the dipole moments (Debye) and vibrational zero-point energies (kcal/mol).

[a] ZPE not included.

[b] The original total energies (hartrees) corresponding to the lowest energy minimum $\mathbf{1}_{\text{s-H}}$ at various levels of theory are (1) −365.729282, (2) −365.7332102, (3) −366.7546057, (4) −366.7581627, (5) −366.8170238, (6) −366.8205173, (7) −366.0484685, and (8) −366.0646696.

TABLE 2 Relative Energies, with ZPE Corrections, for Singlet $\mathbf{1}_{\text{s-Me}}$, $\mathbf{2}_{\text{s-Me}}$, and $\mathbf{3}_{\text{s-Me}}$ as Well as Triplet States $\mathbf{1}_{\text{t-Me}}$, $\mathbf{2}_{\text{t-Me}}$, and $\mathbf{3}_{\text{t-Me}}$ of Silylenic $(CH_3)_2C_2Si$

	Relative Energies (kcal/mol)								*Dipole Moments (D)*	*Vibrational Zero Point Energies (kcal/mol)*
Structure	*HF/ 6-31G**	*HF/ 6-31G***	*B1LYP/ 6-31G**	*B1LYP/ 6-31G***	*B3LYP/ 6-31G**	*B3LYP/ 6-31G***	*MP2/ 6-31G**[a]	*MP2/ 6-31G***[a]	*B3LYP/ 6-31G***	*B3LYP/ 6-31G***
$\mathbf{1}_{\text{s-Me}}$[b]	[1]0.00	[2]0.00	[3]0.00	[4]0.00	[5]0.00	[6]0.00	[7]0.00	[8]0.00	2.22	53.91
$\mathbf{1}_{\text{t-Me}}$	71.93	–	68.70	68.67	68.48	68.46	95.32	95.39	2.24	52.20
$\mathbf{2}_{\text{s-Me}}$	24.71	24.71	19.13	19.11	19.01	18.98	22.66	22.83	2.73	53.86
$\mathbf{2}_{\text{t-Me}}$	32.47	32.52	44.05	44.07	44.73	44.75	58.83	58.87	2.68	53.19
$\mathbf{3}_{\text{s-Me}}$	12.04	11.79	13.90	13.57	14.17	13.84	18.75	18.69	2.44	51.93
$\mathbf{3}_{\text{t-Me}}$	22.42	22.15	40.03	39.53	40.26	39.95	47.38	47.34	1.20	52.30

Relative energies are calculated at six levels of theory: where global minimum is set at 0.00 kcal/mol; along with the dipole moments (Debye) and vibrational zero point energies (kcal/mol).

[a] ZPE not included.

[b] The original total energies (hartrees) corresponding to the lowest energy minimum $\mathbf{1}_{\text{s-Me}}$ at various levels of theory are (1) −443.86134203, (2) −443.8231154, (3) −445.3448983, (4) −445.3534673, (5) −445.463172, (6) −445.4715806, (7) −444.3982581, and (8) −444.446246.

TABLE 3 Relative Energies, with ZPE Corrections, for Singlet $\mathbf{1}_{\text{s-}i\text{-Pro}}$, $\mathbf{2}_{\text{s-}i\text{-Pro}}$, and $\mathbf{3}_{\text{s-}i\text{-Pro}}$ as Well as Triplet States $\mathbf{1}_{\text{t-}i\text{-Pro}}$, $\mathbf{2}_{\text{t-}i\text{-Pro}}$, and $\mathbf{3}_{\text{t-}i\text{-Pro}}$ of Silylenic $((CH_3)_2CH)_2C_2Si$

	Relative Energies (kcal/mol)								*Dipole Moments (D)*	*Vibrational Zero Point Energies (kcal/mol)*
Structure	*HF/ 6-31G**	*HF/ 6-31G***	*B1LYP/ 6-31G**	*B1LYP/ 6-31G**	*B3LYP/ 6-31G**	*B3LYP/ 6-31G***	*MP2/ 6-31G**[a]	*MP2/ 6-31G***[a]	*B3LYP/ 6-31G***	*B3LYP/ 6-31G***
$\mathbf{1}_{\text{s-}i\text{-Pro}}$[b]	[1]0.00	[2]0.00	[3]0.00	[4]0.00	[5]0.00	[6]0.00	[7]0.00	[8]0.00	1.92	125.75
$\mathbf{1}_{\text{t-}i\text{-Pro}}$	59.33	59.28	66.91	51.11	66.65	51.16	–	–	3.44	124.36
$\mathbf{2}_{\text{s-}i\text{-Pro}}$	25.11	25.05	18.55	18.44	18.30	18.15	20.49	20.46	2.64	125.78
$\mathbf{2}_{\text{t-}i\text{-Pro}}$	33.11	33.07	18.55	18.44	43.97	43.83	56.62	56.55	2.89	125.03
$\mathbf{3}_{\text{s-}i\text{-Pro}}$	17.50	17.35	18.57	18.35	18.71	18.48	24.54	24.60	2.51	123.94
$\mathbf{3}_{\text{t-}i\text{-Pro}}$	26.93	26.76	42.90	42.74	43.21	42.99	52.49	52.59	1.27	124.22

Relative energies are calculated at six levels of theory, where global minimum is set at 0.00 kcal/mol; along with the dipole moments (Debye) and vibrational zero point energies (kcal/mol).

[a] ZPE not included.

[b] The original total energies (hartrees) corresponding to the lowest energy minimum $\mathbf{1}_{\text{s-}i\text{-Pr}}$ at various levels of theory are (1) −599.953954, (2) −599.9757206, (3) −602.4907706, (4) −602.5105199, (5) −602.7198822, (6) −602.7392492, (7) −601.0708068, and (8) −601.184429.

TABLE 4 Relative Energies, with ZPE Corrections, for Singlet **1**$_{\text{s-}tert\text{-Bu}}$, **2**$_{\text{s-}tert\text{-Bu}}$, and **3**$_{\text{s-}tert\text{-Bu}}$ as Well as Triplet States **1**$_{\text{t-}tert\text{-Bu}}$, **2**$_{\text{t-}tert\text{-Bu}}$, and **3**$_{\text{t-}tert\text{-Bu}}$ of Silylenic $((CH_3)_3C)_2C_2Si$

	Relative Energies (kcal/mol)								*Dipole Moments (D)*	*Vibrational Zero Point Energies (kcal/mol)*
Structure	*HF/ 6-31G**	*HF/ 6-31G***	*B1LYP/ 6-31G**	*B1LYP/ 6-31G***	*B3LYP/ 6-31G**	*B3LYP/ 6-31G***	*MP2/ 6-31G*[a]*	*MP2/ 6-31G**[a]*	*B3LYP/ 6-31G***	*B3LYP/ 6-31G***
1$_{\text{s-}tert\text{-Bu}}$[b]	[1]0.00	[2]0.00	[3]0.00	[4]0.00	[5]0.00	[6]0.00	[7]0.00	[8]0.00	2.06	160.66
1$_{\text{t-}tert\text{-Bu}}$	38.01	0.46	47.31	47.29	47.47	47.46	51.33	–	3.56	159.40
2$_{\text{s-}tert\text{-Bu}}$	35.14	38.61	27.26	27.11	26.96	26.79	29.08	–	2.60	161.29
2$_{\text{t-}tert\text{-Bu}}$	39.47	39.48	48.91	50.70	49.39	49.28	62.34	–	2.90	160.47
3$_{\text{s-}tert\text{-Bu}}$	13.46	13.38	15.39	15.37	15.67	15.66	23.01	–	2.49	158.98
3$_{\text{t-}tert\text{-Bu}}$	22.69	22.61	39.46	39.46	39.84	39.84	51.13	–	1.30	159.10

Relative energies are calculated at six levels of theory, where global minimum is set at 0.00 kcal/mol, along with the dipole moments (Debye) and vibrational zero point energies (kcal/mol).

[a] ZPE not included.

[b] The original total energies (hartrees) corresponding to the lowest energy minimum **1**$_{\text{s-}tert\text{-Bu}}$ at various levels of theory are (1) −678.0140314, (2) −678.0419616, (3) −681.0568103, (4) −681.0822781, (5) −681.3415374, (6) −681.3665905, (7) −679.4088679 and (8) −. . . .

of bond dissociation energies, heats of formation, and geometrical parameters. Among all DFT methods, B3LYP often gives geometries and vibrational frequencies which are closest to those obtained from the MP2 method. Thus, B3LYP with the 6-31G** basis set is employed, as the method of choice, for being fairly good in correlation with previously published results [37–40].

Hence, in this work B3LYP/6-31G** results are preferred over other calculation methods. All methods of calculation introduce **1**$_{\text{s-X}}$ as the global minima. For the sake of convenience, these global minima are assigned a relative energy value of 0.00 kcal/mol (Tables 1–4). Structural parameters for different isomers of X_2C_2Si are reported using B3LYP/6-31G** and MP2/6-31G** (Fig. 2). In order to clarify the stereochemical and symmetrical features of our optimized structures, the B3LYP/6-31G** calculated structures of 24 X_2C_2Si species are also presented using balls and cylinders model (Fig. 3). Optimized geometrical parameters obtained through methods other than B3LYP/6-31G** and MP2/6-31G** show similar trends, and for the sake of clarity they are omitted from Fig. 2. Linear correlations are encountered between the LUMO–HOMO energy gaps of the singlet X_2C_2Si silylenes (**1**$_{\text{s-X}}$ and **2**$_{\text{s-X}}$), and their corresponding singlet–triplet energy separations are calculated at B3LYP/6-31G** level of theory (Fig. 4). The linearity trend is **2**$_{\text{s-X}}$ ($R^2 = 0.99$) > **1**$_{\text{s-X}}$ ($R^2 = 0.68$) > **3**$_{\text{s-X}}$ ($R^2 = 0.20$), where R^2 is a correlation coefficient. In the cyclic structures, such as **1**$_{\text{s-X}}$, a small change in the LUMO–HOMO energy gaps (7–8 kcal/mol) makes large changes in their corresponding $\Delta E_{\text{s-t,X}}$ (30–32 kcal/mol). It is in contrast to the acyclic structures, such as **2**$_{\text{s-X}}$, where changes in the $\Delta E_{\text{s-t,X}}$ as a function of LUMO–HOMO energy gaps are rather insignificant. One of the significant parameters that affected $\Delta E_{\text{s-t}}$ and determination of the ground-state of divalent carbene like species is the magnitude of the divalent bond angle [40]. Therefore, bending potential energy curves for divalent structures **3**$_{\text{s-X}}$ and **3**$_{\text{t-X}}$ are calculated at B3LYP/6-31G** (Fig. 5). The singlet state **3**$_{\text{s-H}}$ and triplet state **3**$_{\text{t-H}}$ cross at ∠HSiC divalent angle about 133°. Interestingly, when hydrogen atom is replaced by the larger alkyl groups, changes in the cross-points (about 140°) are very little. This finding indicates that steric effects of substituents X employed are not much of significance in the singlet–triplet energy separations of X_2C_2Si [4]. The B3LYP/6-31G** IR spectral data, involving selected harmonic frequencies (cm^{-1}) and IR intensities (km/mol) for all 24 silylenic isomers scrutinized, are presented (Tables 5–8). This calculation assists us to estimate the zero-point vibrational energy correction and allows an assessment of the nature of stationary points on their potential energy surfaces. Force constant calculations show that in the X_2C_2Si series (where X is methyl and/or *tert*-butyl) **2**$_{\text{s-Me}}$, **2**$_{\text{t-Me}}$, **3**$_{\text{s-Me}}$, **1**$_{\text{t-Me}}$, **1**$_{\text{s-Me}}$, **1**$_{\text{s-}tert\text{-Bu}}$, and **3**$_{\text{t-}tert\text{-Bu}}$ possess negative force constants so these are not real isomers on the energy surface of X_2C_2Si silylenes (Tables 5–8). Lastly, the NBO analysis including atomic charges of 24 structures considered in this study was done at B3LYP/6-31G** (Table 9).

Considering the above results, three key issues are discussed below: First, the relative stability among three isomeric sets of X_2C_2Si, second singlet–triplet energy separation comparisons between isomers in each structure, and third geometries, symmetries, force constants, dipole moments, and charges in each isomeric series.

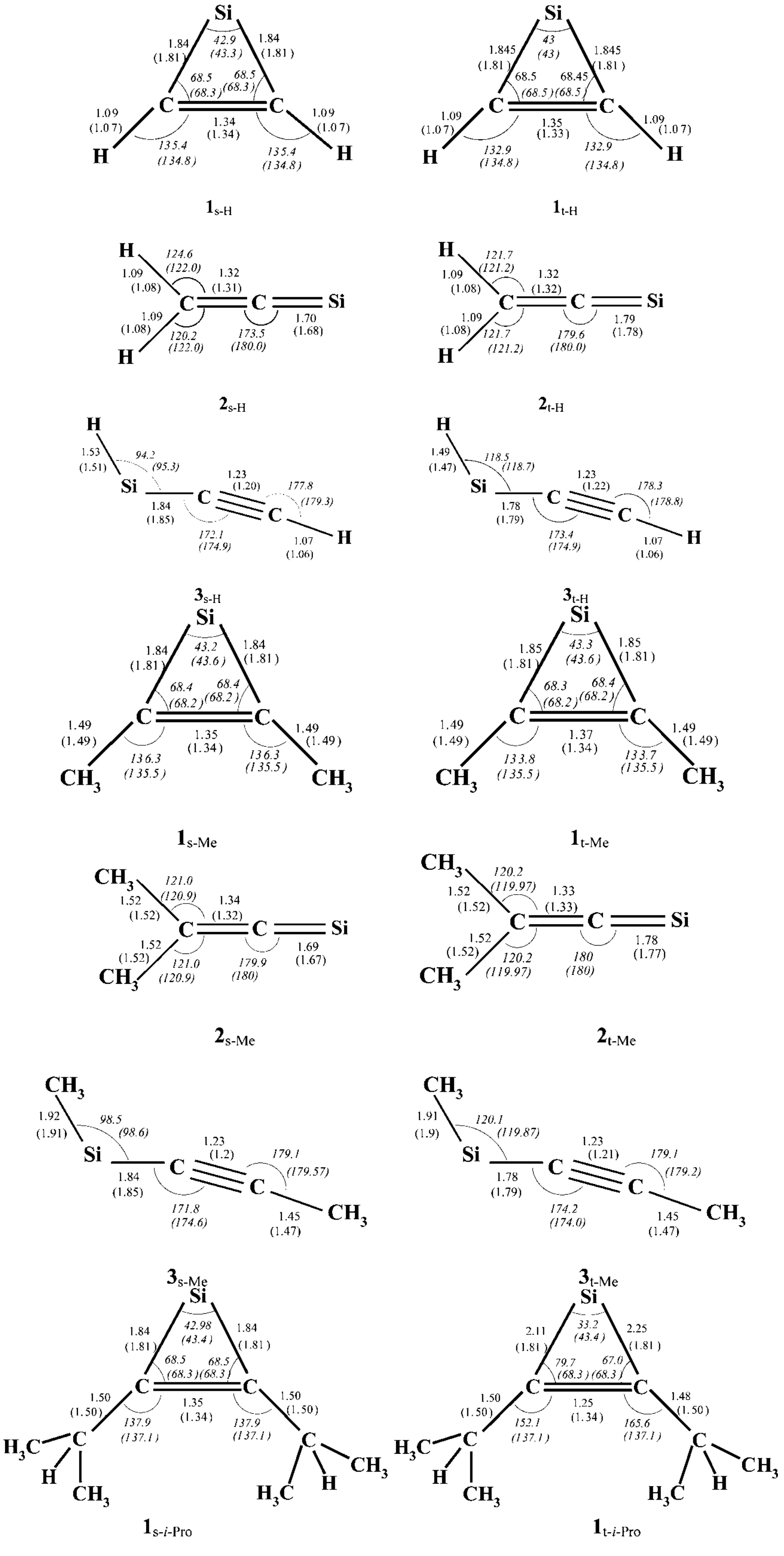

FIGURE 2 Geometrical parameters of 24 silylenic X_2C_2Si (where X is H, Me, *i*-Pro, and *tert*-Bu) with bond lengths (in angstroms) and *bond angles* (in degrees) optimized at B3LYP/6-31G** and HF/ 6-31 + G** (within parentheses).

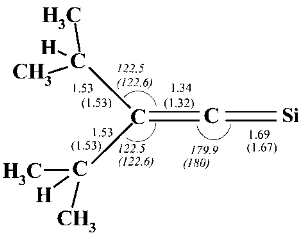

2$_{\text{s-}i\text{-Pro}}$

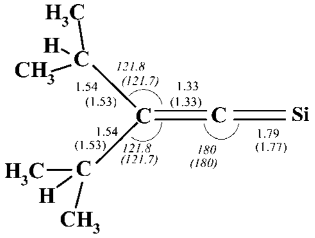

2$_{\text{t-}i\text{-Pro}}$

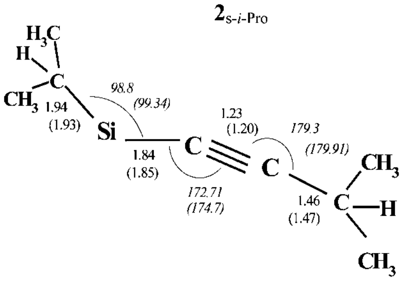

3$_{\text{s-}i\text{-Pro}}$

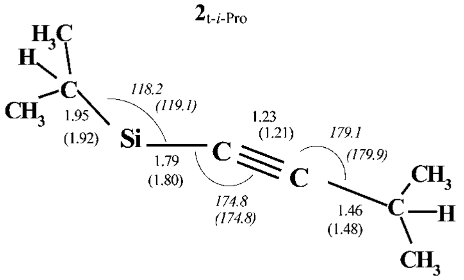

3$_{\text{t-}i\text{-Pro}}$

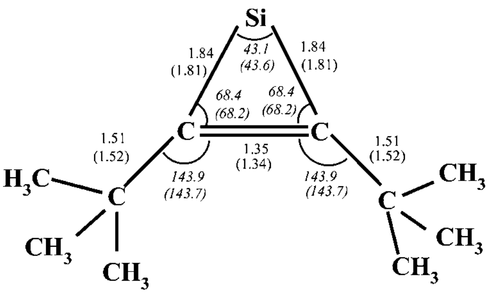

1$_{\text{s-}tert\text{-Bu}}$

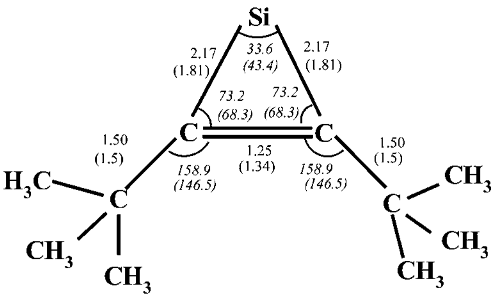

1$_{\text{t-}tert\text{-Bu}}$

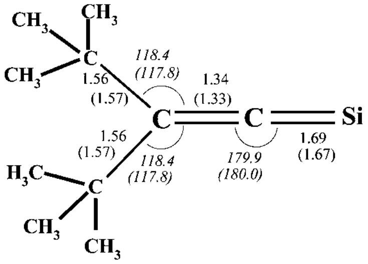

2$_{\text{s-}tert\text{-Bu}}$

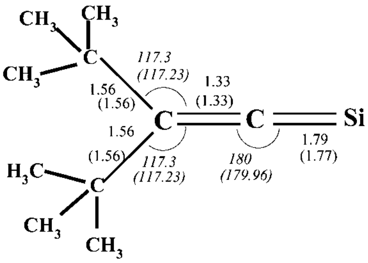

2$_{\text{t-}tert\text{-Bu}}$

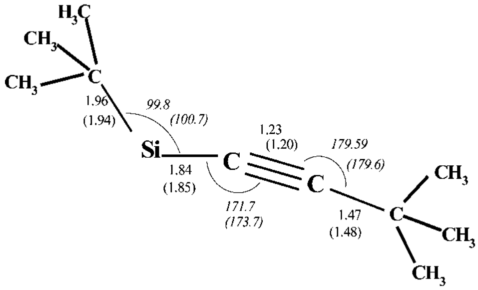

3$_{\text{s-}tert\text{-Bu}}$

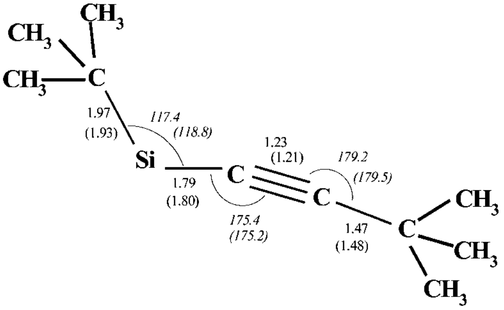

3$_{\text{t-}tert\text{-Bu}}$

FIGURE 2 Continued

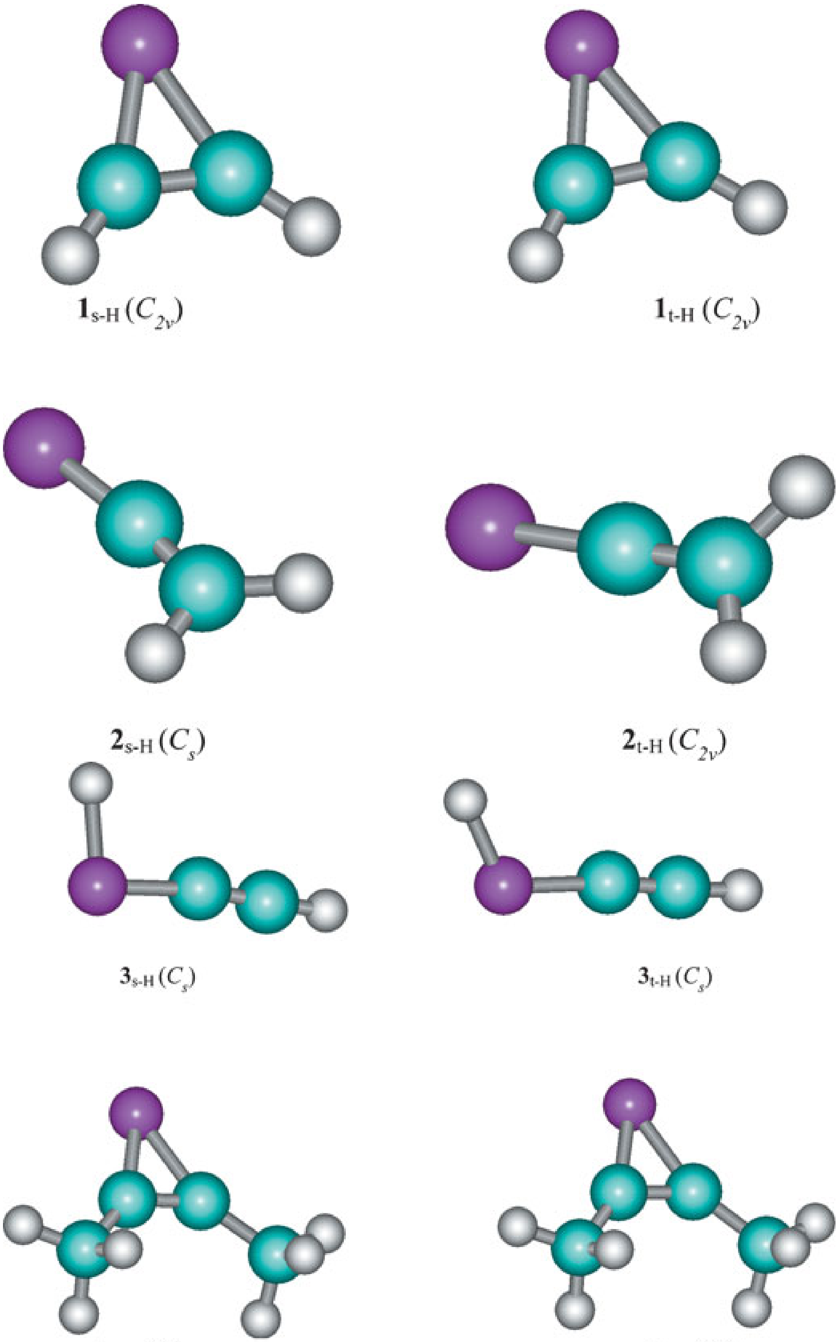

$\mathbf{1}_{s\text{-}H}$ (C_{2v}) $\mathbf{1}_{t\text{-}H}$ (C_{2v})

$\mathbf{2}_{s\text{-}H}$ (C_s) $\mathbf{2}_{t\text{-}H}$ (C_{2v})

$\mathbf{3}_{s\text{-}H}$ (C_s) $\mathbf{3}_{t\text{-}H}$ (C_s)

$\mathbf{1}_{s\text{-}Me}$ (C_s) $\mathbf{1}_{t\text{-}Me}$ (C_s)

FIGURE 3 Balls and cylinders model of optimized structures along with the symmetries for 24 silylenic X_2C_2Si structures at B3LYP/6-31G** (where X is H, Me, *i*-Pro, *tert*-Bu).

Relative Stability

B3LYP/6-31G** calculated relative stability for H_2C_2Si isomers is $\mathbf{1}_{s\text{-}H}$ (0.00 kcal/mol) > $\mathbf{2}_{s\text{-}H}$ (15.36 kcal/mol) > $\mathbf{3}_{s\text{-}H}$ (20.85 kcal/mol) > $\mathbf{2}_{t\text{-}H}$ (36.99 kcal/mol) $\mathbf{3}_{t\text{-}H}$ (44.54 kcal/mol) > $\mathbf{1}_{t\text{-}H}$ (71.06 kcal/mol) (Table 1). This is in contrast to C_3H_2 carbenic analogues that acyclic triplet state propargylene is more stable than singlet state vinylidenecarbene [41]. It is due to the intrinsic tendency of silylenes for singlet ground states [4]. The structure of the lowest energy and presumably the global minimum of the energy

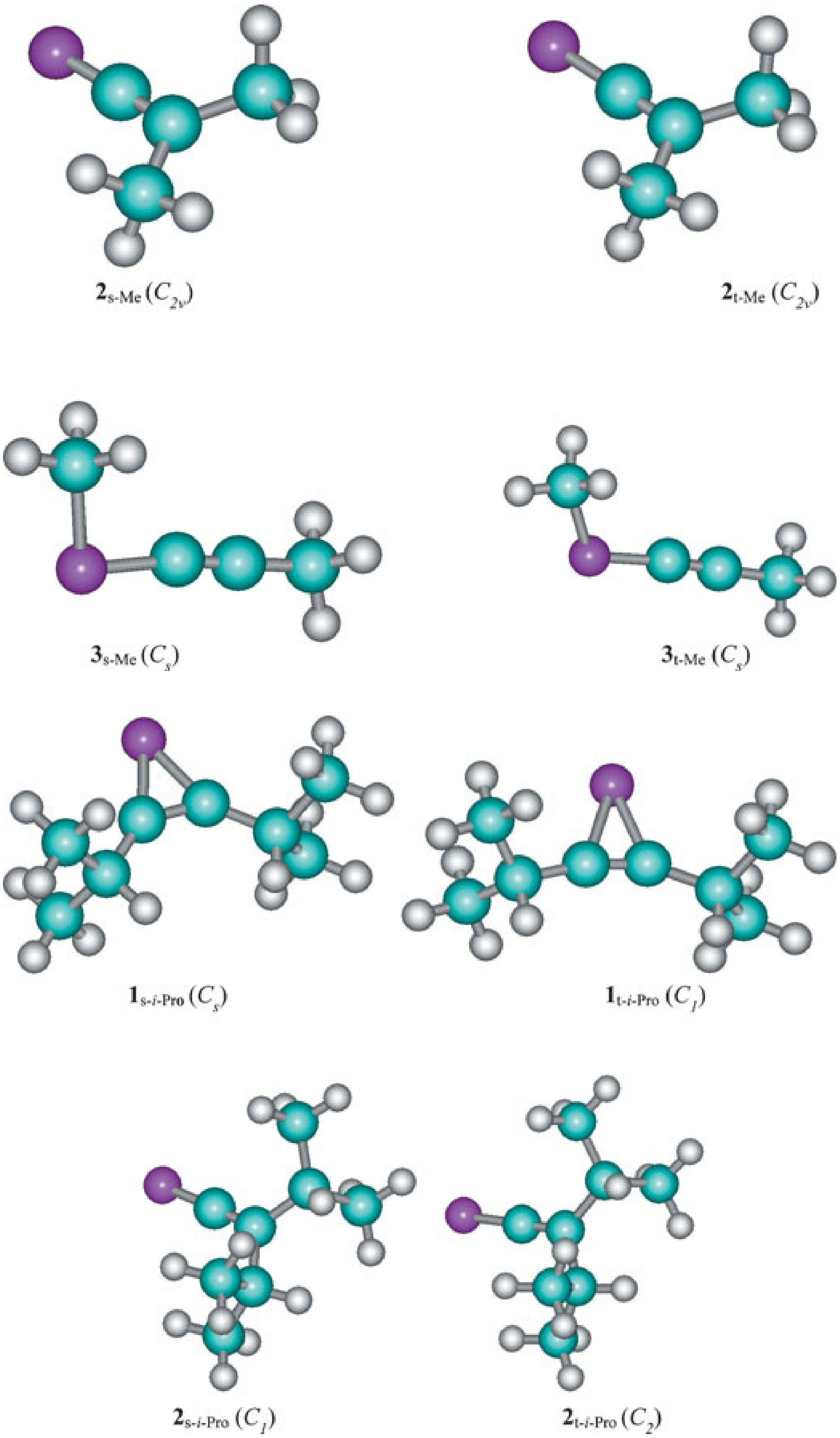

2$_{\text{s-Me}}$ (C_{2v}) **2**$_{\text{t-Me}}$ (C_{2v})

3$_{\text{s-Me}}$ (C_s) **3**$_{\text{t-Me}}$ (C_s)

1$_{\text{s-}i\text{-Pro}}$ (C_s) **1**$_{\text{t-}i\text{-Pro}}$ (C_1)

2$_{\text{s-}i\text{-Pro}}$ (C_1) **2**$_{\text{t-}i\text{-Pro}}$ (C_2)

FIGURE 3 Continued

surface of H_2C_2Si at B3LYP, B1LYP, MP2, and HF emerges as a singlet silacyclopropenylidene, **1**$_{\text{s-H}}$. Obviously, **1**$_{\text{s-H}}$ has a great stabilization σ^2 silylenic center which enables it to show an aromatic character. Hence, **2**$_{\text{s-H}}$ is less stable than **1**$_{\text{s-H}}$, due to its lack of the aromatic character. **2**$_{\text{s-H}}$ is more stable than **3**$_{\text{s-H}}$. This finding can be attributed to the fact that **2**$_{\text{s-H}}$ has an ally cationic canonical form but **3**$_{\text{s-H}}$ has a vinyl cationic form [3]. This justification can also be applied to the stability of **2**$_{\text{t-H}}$ over **3**$_{\text{t-H}}$; that allylic

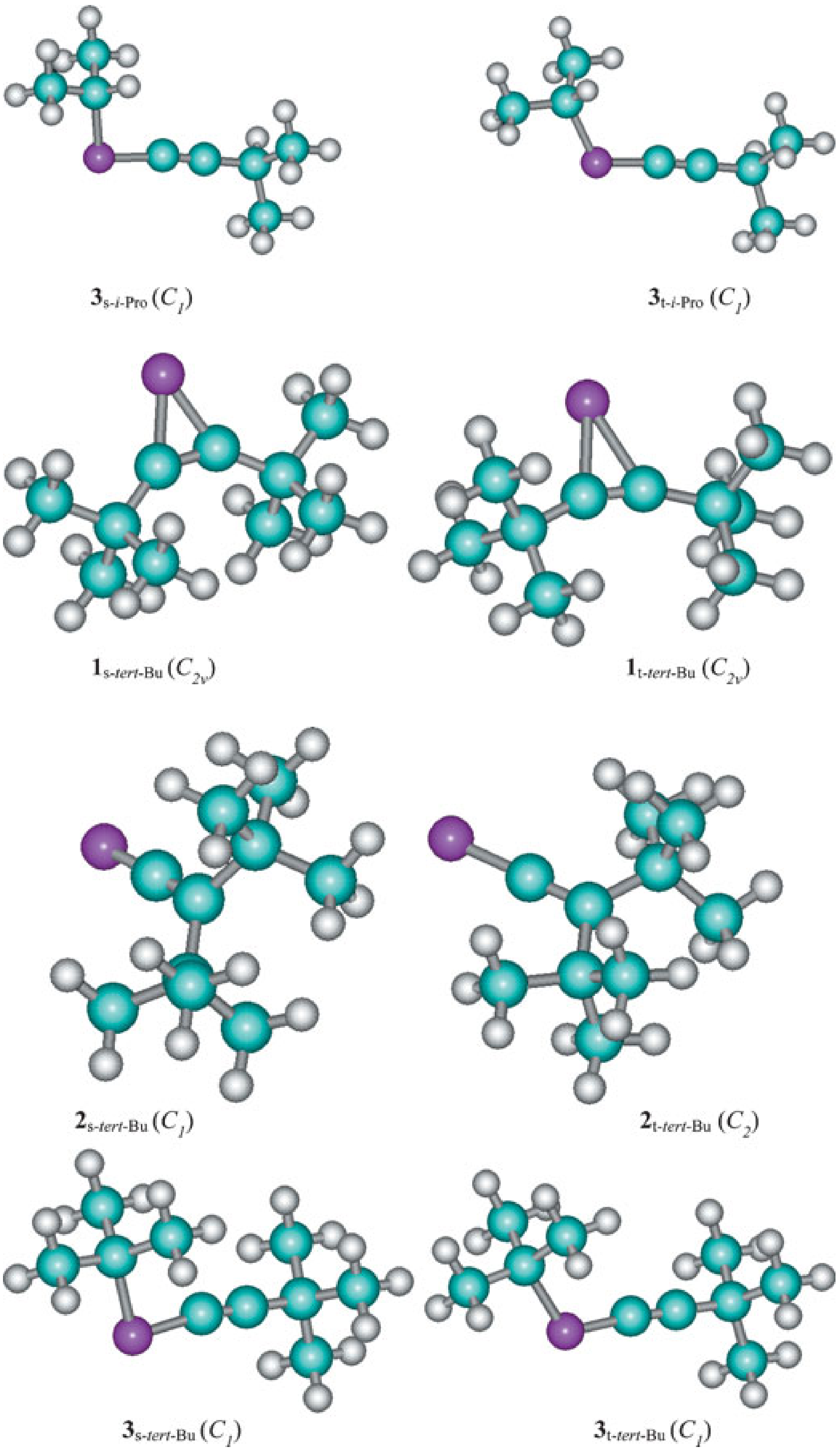

$\mathbf{3}_{\text{s-}i\text{-Pro}}$ (C_1)

$\mathbf{3}_{\text{t-}i\text{-Pro}}$ (C_1)

$\mathbf{1}_{\text{s-}tert\text{-Bu}}$ (C_{2v})

$\mathbf{1}_{\text{t-}tert\text{-Bu}}$ (C_{2v})

$\mathbf{2}_{\text{s-}tert\text{-Bu}}$ (C_1)

$\mathbf{2}_{\text{t-}tert\text{-Bu}}$ (C_2)

$\mathbf{3}_{\text{s-}tert\text{-Bu}}$ (C_1)

$\mathbf{3}_{\text{t-}tert\text{-Bu}}$ (C_1)

FIGURE 3 Continued

and/or vinylic radicals are presented. Finally, due to enormous angle strains in the three-membered ring $\mathbf{1}_{\text{t-H}}$ turns out to be the least stable isomer in the H_2C_2Si series. B3LYP/6-31G** calculated order of relative stability for $(CH_3)_2C_2Si$ structures is $\mathbf{1}_{\text{s-Me}}$ (0.00 kcal/mol) > $\mathbf{3}_{\text{s-Me}}$ (13.84 kcal/mol) > $\mathbf{2}_{\text{s-Me}}$ (18.98 kcal/mol) > $\mathbf{3}_{\text{t-Me}}$ (39.95 kcal/mol) > $\mathbf{2}_{\text{t-Me}}$ (44.74 kcal/mol) > $\mathbf{1}_{\text{t-Me}}$ (68.45 kcal/mol) (Table 2). This is clear that the stability order of $(CH_3)_2C_2Si$ appears somewhat different from the above stability

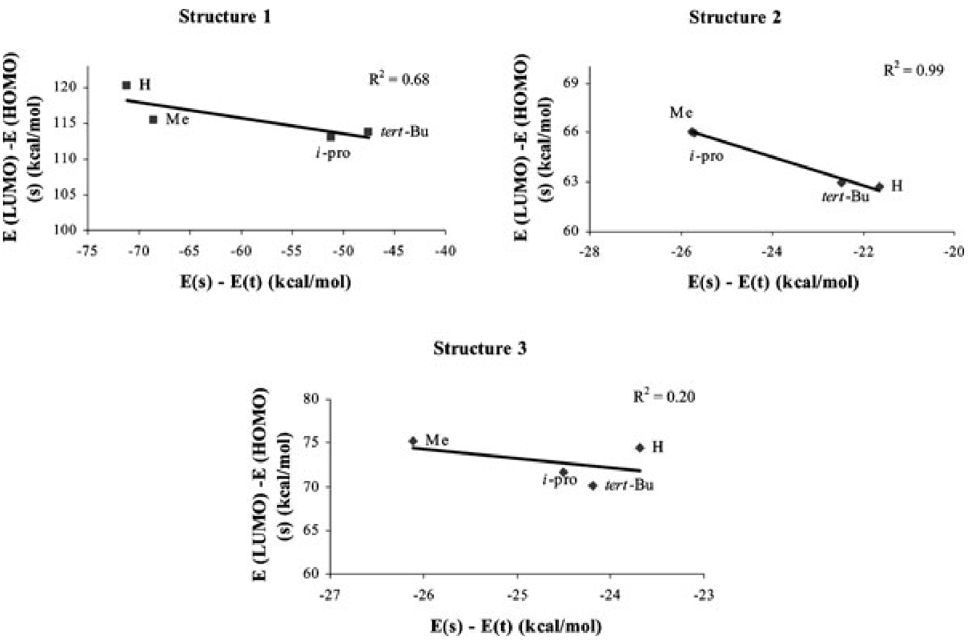

FIGURE 4 Correlations between the LUMO–HOMO energy gaps of the singlet X_2C_2Si silylenes ($\mathbf{1}_{\text{s-X}}$, $\mathbf{2}_{\text{s-X}}$ and $\mathbf{3}_{\text{s-X}}$), and their corresponding singlet–triplet energy separations, E (**s**)–E (**t**) ($-\Delta E_{\text{s-t,X}}$), for X = H, Me, *i*-pro, and *tert*-Bu calculated at B3LYP/6-31G** level of theory (R^2 is the correlation coefficient).

trend of H_2C_2Si. Replacing of the stability order of $\mathbf{2}_{\text{s-Me}}$ and $\mathbf{2}_{\text{t-Me}}$ with $\mathbf{3}_{\text{s-Me}}$ and $\mathbf{3}_{\text{t-Me}}$ may be attributed to the steric hindrance involved in the structure **2** that both substituents are located on the same carbon. The structure of the lowest energy for the set of $(CH_3)_2C_2Si$ silylenes appears to be a singlet saddle point $\mathbf{1}_{\text{s-Me}}$ (Table 6).

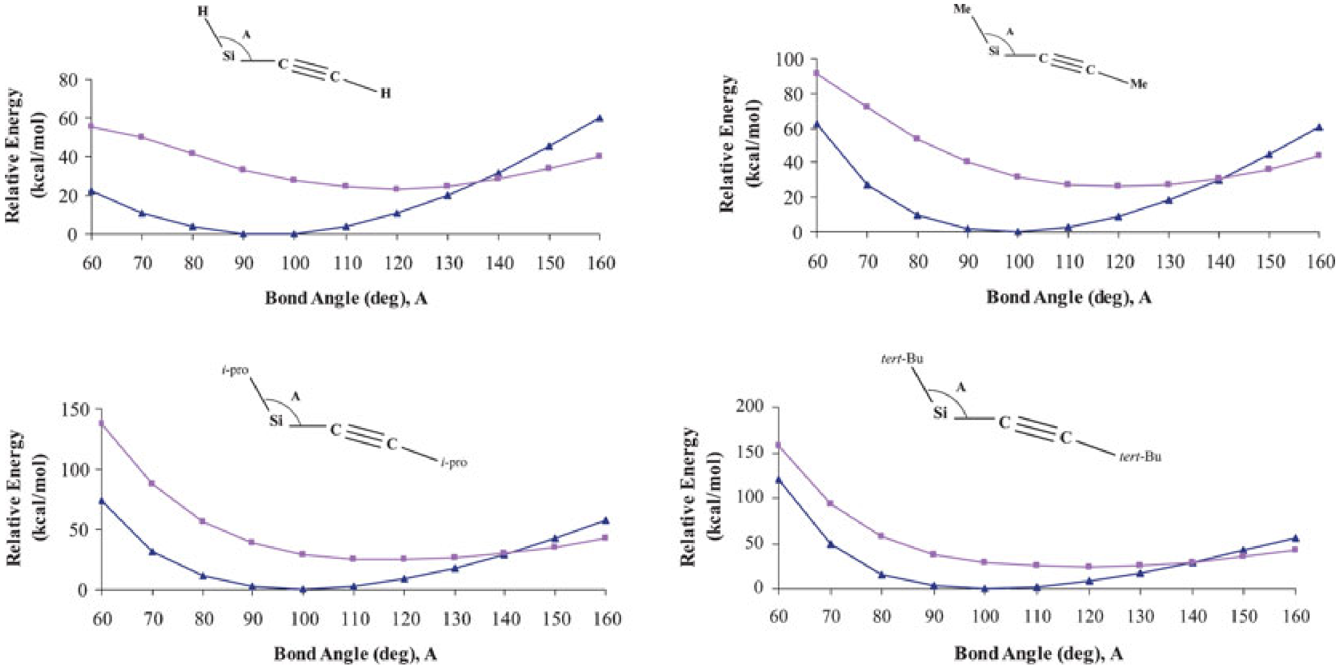

FIGURE 5 B3LYP/6-31G** relative energies (kcal/mol) of the singlet (▲) and triplet (■) states of X-ethynylsilylene, $\mathbf{3}_{\text{s-X}}$ and $\mathbf{3}_{\text{t-X}}$, species plotted as a function of the divalent bond angle ∠XSiC, A (deg) (where X is H, Me, *i*-pro, and *tert*-Bu).

TABLE 5 Selected B3LYP/6-31G** Calculated Harmonic Frequencies (cm^{-1}) and IR Intensities (km/mol; in parenthesis), for Silylenic Isomers, H_2C_2Si

	$\mathbf{1}_{s\text{-}H}$	$\mathbf{1}_{t\text{-}H}$	$\mathbf{2}_{s\text{-}H}$	$\mathbf{2}_{t\text{-}H}$	$\mathbf{3}_{s\text{-}H}$	$\mathbf{3}_{t\text{-}H}$
v_1	670.49(36.3)	243.35(23.7)	217.92(2.1)	234.93(0.8)	201.69(4.3)	249.33(6.0)
v_2	701.43(53.5)	571.06(68.2)	278.59(20.1)	310.53(4.5)	255.86(3.8)	299.93(6.8)
v_3	768.79(36.7)	682.85(27.4)	756.29(17.9)	633.06(6.8)	577.49(46.2)	526.05(44.1)
v_4	902.84(3.2)	737.17(6.6)	994.57(21.5)	755.99(55.5)	614.12(62.1)	666.28(12.0)
v_5	1004.16(0.0)	918.21(9.8)	1021.88(6.9)	842.01(1.3)	758.38(22.9)	683.09(7.3)
v_6	1112.08(52.8)	943.26(0.0)	1446.28(0.6)	1361.50(0.0)	834.29(110.3)	704.83(73.0)
v_7	1513.38(0.1)	1468.52(11.0)	1748.10(52.7)	1602.25(95.3)	2035.64(284.5)	2016.11(13.2)
v_8	3174.73(10.5)	3177.42(2.6)	3079.43(38.5)	3111.50(7.0)	2081.68(68.2)	2179.98(60.9)
v_9	3198.61(10.7)	3204.38(10.8)	3145.39(8.2)	3182.49(0.2)	3465.38(40.6)	3466.81(62.8)

TABLE 6 Selected B3LYP/6-31G** Calculated Harmonic Frequencies (cm^{-1}) and IR Intensities (km/mol; in parenthesis), for Silylenic Structures, $(CH_3)_2C_2Si$

	$\mathbf{1}_{s\text{-}Me}$	$\mathbf{1}_{t\text{-}Me}$	$\mathbf{2}_{s\text{-}Me}$	$\mathbf{2}_{t\text{-}Me}$	$\mathbf{3}_{s\text{-}Me}$	$\mathbf{3}_{t\text{-}Me}$
v_1	–73.80(1.1)	–141.85(0.0)	–199.25(0.0)	–177.61(0.0)	–15.24(0.0)	9.55(0.5)
v_2	–30.43(0.0)	–122.97(0.0)	–169.03(1.9)	–170.27(0.6)	71.58(0.1)	77.42(0.3)
v_3	181.17(0.0)	–89.46(0.8)	143.71(1.2)	108.74(0.2)	94.89(1.6)	92.59(2.5)
v_4	252.90(3.2)	185.59(0.5)	159.73(1.7)	189.04(1.6)	122.46(1.3)	163.96(4.7)
v_5	328.73(4.3)	200.07(4.5)	365.34(0.2)	338.76(0.1)	261.19(8.6)	242.71(7.3)
v_6	482.50(0.0)	324.33(8.0)	506.83(0.1)	460.13(0.2)	390.67(0.4)	353.46(0.0)
v_7	625.87(17.0)	448.47(0.0)	543.88(23.0)	471.55(0.7)	393.92(1.7)	400.71(1.2)
v_8	638.12(2.0)	594.74(3.2)	634.19(11.0)	580.26(3.1)	514.60(52.0)	512.75(3.5)
v_9	889.19(15.9)	872.84(1.1)	910.59(0.50)	866.06(2.0)	593.89(1.5)	673.33(27.1)

TABLE 7 Selected B3LYP/6-31G** Calculated Harmonic Frequencies (cm^{-1}) and IR Intensities (km/mol; in parenthesis), for Silylenic Isomers, $((CH_3)_2CH)_2C_2Si$

	$\mathbf{1}_{s\text{-}i\text{-}Pr}$	$\mathbf{1}_{t\text{-}i\text{-}Pr}$	$\mathbf{2}_{s\text{-}i\text{-}Pr}$	$\mathbf{2}_{t\text{-}i\text{-}Pr}$	$\mathbf{3}_{s\text{-}i\text{-}Pr}$	$\mathbf{3}_{t\text{-}i\text{-}Pr}$
v_1	18.16(0.3)	25.26(0.6)	25.72(0.1)	35.99(0.2)	21.21(0.1)	19.93(0.3)
v_2	27.94(0.0)	32.60(0.2)	68.39(0.0)	62.96(0.0)	24.58(0.3)	26.80(0.4)
v_3	96.24(0.0)	86.34(4.2)	106.00(0.1)	79.49(0.3)	50.71(0.4)	48.04(0.6)
v_4	130.68(0.0)	105.31(0.1)	115.90(0.1)	125.55(0.1)	93.28(0.1)	106.91(0.9)
v_5	170.77(0.0)	114.32(4.0)	185.15(0.1)	168.83(0.2)	132.16(0.6)	123.81(0.6)
v_6	193.47(0.2)	173.67(0.0)	224.11(0.2)	231.65(0.0)	179.25(1.1)	227.96(0.4)
v_7	236.78(0.0)	183.19(1.7)	228.05(0.3)	233.55(0.0)	217.95(0.1)	230.13(0.0)
v_8	237.36(0.0)	216.82(0.1)	253.79(0.5)	256.37(0.0)	225.22(0.6)	237.42(0.0)
v_9	254.50(0.2)	223.37(0.1)	258.36(0.0)	258.88(0.2)	229.21(0.0)	250.06(0.2)

TABLE 8 Selected B3LYP/6-31G** Calculated Harmonic Frequencies (cm^{-1}) and IR Intensities (km/mol; in parenthesis), for Silylenic Structures, $((CH_3)_3C)_2C_2Si$

	$\mathbf{1}_{s\text{-}t\text{-}Bu}$	$\mathbf{1}_{t\text{-}t\text{-}Bu}$	$\mathbf{2}_{s\text{-}t\text{-}Bu}$	$\mathbf{2}_{t\text{-}t\text{-}Bu}$	$\mathbf{3}_{s\text{-}t\text{-}Bu}$	$\mathbf{3}_{t\text{-}t\text{-}Bu}$
v_1	–48.46(0.0)	19.56(0.0)	20.96(0.1)	37.94(0.3)	12.92(0.0)	–8.03(0.3)
v_2	23.30(0.1)	35.89(1.1)	99.23(0.0)	88.27(0.3)	21.76(0.5)	24.27(0.2)
v_3	135.06(0.0)	56.27(7.8)	120.02(0.2)	91.97(0.0)	48.96(0.3)	40.54(0.5)
v_4	139.58(0.0)	92.49(0.2)	149.22(0.1)	157.76(0.2)	77.51(0.0)	87.14(0.4)
v_5	183.83(0.0)	112.62(0.0)	204.09(0.1)	208.11(0.0)	129.68(0.4)	117.07(0.4)
v_6	186.05(0.2)	159.06(0.0)	222.38(0.0)	219.90(0.1)	159.45(0.8)	216.34(0.5)
v_7	208.13(0.0)	171.88(0.0)	238.21(0.1)	243.26(0.0)	221.85(0.4)	227.42(0.0)
v_8	235.11(0.0)	221.40(0.0)	263.16(0.3)	276.01(0.2)	225.45(0.4)	239.06(0.1)
v_9	259.02(0.1)	224.87(0.2)	266.84(0.3)	277.66(0.1)	225.58(0.3)	249.15(0.30)

The B3LYP/6-31G** calculated order of relative stability for $((CH_3)_2CH)_2C_2Si$ isomers is **1**$_{\text{s-}i\text{-pro}}$ (0.00 kcal/mol) > **2**$_{\text{s-}i\text{-pro}}$ (18.14 kcal/mol) ≈ **3**$_{\text{s-}i\text{-pro}}$ (18.47 kcal/mol) > **3**$_{\text{t-}i\text{-pro}}$ (43.00 kcal/mol) ≈ **2**$_{\text{t-}i\text{-pro}}$ (43.83 kcal/mol) > **1**$_{\text{t-}i\text{-pro}}$ (51.15 kcal/mol) (Table 3). This is roughly the same trend found for $(CH_3)_2C_2Si$, but with decrease in the energy difference between **2**$_{\text{s-}i\text{-pro}}$ and **3**$_{\text{s-}i\text{-pro}}$. One may justify this phenomenon by considering the stereochemistry of these isomers (Fig. 3). Interestingly, both **2**$_{\text{s-}i\text{-pro}}$ and **3**$_{\text{s-}i\text{-pro}}$ have C_1 symmetry, so this decrease in the symmetry, in turn decreases the steric hindrance in structure **2**$_{\text{s-}i\text{-pro}}$; while in **2**$_{\text{s-Me}}$ existence of two planes of symmetry (C_{2v}) makes an eclipsed conformation. The global minimum for the set of $((CH_3)_2CH)_2C_2Si$ isomers appears to be singlet cyclic **1**$_{\text{s-}i\text{-pro}}$ (Table 3).

The B3LYP/6-31G** calculated order of relative stability for $((CH_3)_3C)_2C_2Si$ structures is **1**$_{\text{s-}tert\text{-Bu}}$ (0.00 kcal/mol) > **3**$_{\text{s-}tert\text{-Bu}}$ (15.66 kcal/mol) > **2**$_{\text{s-}tert\text{-Bu}}$ (26.79 kcal/mol) > **3**$_{\text{t-}tert\text{-Bu}}$ (39.84 kcal/mol) > **1**$_{\text{t-}tert\text{-Bu}}$ (47.46 kcal/mol) > **2**$_{\text{t-}tert\text{-Bu}}$ (49.28 kcal/mol) (Table 4). This is almost the same trend found for $(CH_3)_2C_2Si$, but with a displacement in the stability order of **1**$_{\text{t-}tert\text{-Bu}}$ instead **2**$_{\text{t-}tert\text{-Bu}}$. The least sterically hindered, open chain, fully staggered **3**$_{\text{s-}tert\text{-Bu}}$ with C_1 symmetry, appears to be more stable than the **2**$_{\text{s-}tert\text{-Bu}}$ (Fig. 3). It is notable that the transition state **1**$_{\text{s-}tert\text{-Bu}}$ with excessive angle strains and crowding of the two large *tert*-butyl groups has yet a large amount of stability and appears as the structure of the lowest energy in the set of $((CH_3)_3C)_2C_2Si$ (Table 8).

Singlet–Triplet Energy Separations Comparison

Inspection of cyclic silylenes revealed that singlet silacyclopropenylidenes, **1**$_{\text{s-X}}$, appear more stable than their corresponding triplet states, $1_{\text{t-X}}$, due to the lack of aromatic character and angle-strains involved in $1_{\text{t-X}}$ (Tables 1–4). These results are consistent with those reported for analogues carbenic X_2C_3 and some related systems [3,9,21,42]. The B3LYP/6-31G** calculated order of singlet–triplet energy gaps ($\Delta E_{\text{s-t,X}}$) between **1**$_{\text{s-X}}$ and **1**$_{\text{t-X}}$ is $\Delta E_{\text{s-t,H}}$ (71.068 kcal/mol) > $\Delta E_{\text{s-t,Me}}$ (68.45 kcal/mol) > $\Delta E_{\text{s-t,}i\text{-Pro}}$ (51.15 kcal/mol) > $\Delta E_{\text{s-t,}tert\text{-Bu}}$ (47.46 kcal/mol) (Tables 1–4). In the cyclic structure **1**$_{\text{X}}$, the magnitude of $\Delta E_{\text{s-t,X}}$ is inversely proportional to the size of X. The stability of the triplet state $1_{\text{t-X}}$ increases as a function of the size of substituent (X) (Tables 1–4). The secondary carbocation pertaining to canonical form "b" of **1**$_{\text{s-H}}$, with a relative stability of 0.00 kcal/mol, appears to be 49,353 kcal/mol less stable than the corresponding tertiary carbocation in **1**$_{\text{s-Me}}$ (Scheme 1). Likewise, the secondary radical of canonical form "b′" of **1**$_{\text{t-H}}$, with a relative stability of 0.00 kcal/mol, is 55,631 kcal/mol less stable than the tertiary radical in **1**$_{\text{t-Me}}$. The higher relative sensitivity of the triplet state to methyl group, compared to hydrogen, is attributed to the lower importance of the canonical form "b′" in **1**$_{\text{s-H}}$, due to the separation of charge (Scheme 1). This finding is in agreement with the well-documented data on stabilization of triplet silylenes [3–5]. Moreover, hyperconjugation justifies the higher relative sensitivity of the singlet **1**$_{\text{s-X}}$ over the corresponding triplet state **1**$_{\text{t-X}}$ when X is *i*-pro. When X is *tert*-Bu, similar magnitudes of sensitivity are displayed by both singlet **1**$_{\text{s-X}}$ and triplet **1**$_{\text{t-X}}$ (Scheme 1).

The first acyclic structure considered is 3,3-diX-vinylidenesilylene, **2**$_{\text{X}}$ (Fig. 1). All singlet states **2**$_{\text{s-X}}$ appear more stable than their corresponding triplet states **2**$_{\text{t-X}}$ (Tables 1–4). The order of energy gaps between **2**$_{\text{s-X}}$ and **2**$_{t\text{-}X}$ ($\Delta E_{\text{s-t,X}}$) calculated at the B3LYP/6-31G** level is $\Delta E_{\text{s-t,Me}}$ (25.76 kcal/mol) ≈ $\Delta E_{\text{s-t,}i\text{-Pro}}$ (25.68 kcal/mol) > $\Delta E_{\text{s-t,}tert\text{-Bu}}$ (22.48 kcal/mol) > $\Delta E_{\text{s-t,H}}$(21.64 kcal/mol) (Tables 1–4). These results clearly demonstrate that the $\Delta E_{\text{s-t,X}}$ in structure **2**$_{\text{X}}$ is lower than those of structure **1**$_{\text{X}}$; in addition changes in $\Delta E_{\text{s-t,X}}$ as a function of X is very small (4.12 kcal/mol). This can be attributed to the lack of such aromatic character that exists in the structure **1**$_{\text{X}}$.

In discussing silylenes with acyclic structures, the last appears to be ethynylsilylene, **3** (Fig. 1). Again, all singlet states **3**$_{\text{s-X}}$ appear more stable than their corresponding triplet states **3**$_{\text{t-X}}$

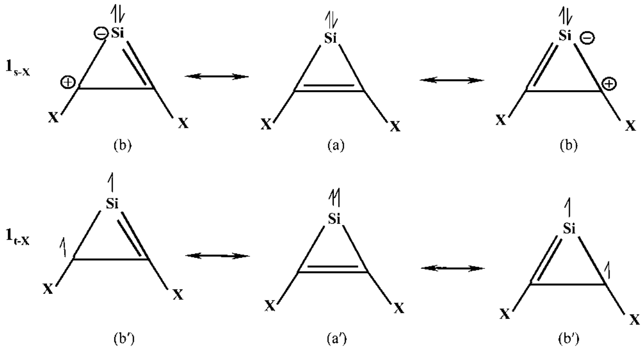

SCHEME 1 Effects of substituents (X) on the relative stability of significant canonical forms of singlet **1**$_{\text{s-X}}$ (a vs. b) and triplet **1**$_{\text{t-X}}$ (a′ vs. b′) for X = H, Me, *i*-pro, and *tert*-Bu. Relative absolute energies (kcal/mol) for **1**$_{\text{s-X}}$ series are **1**$_{\text{s-H}}$ = 197,374, **1**$_{\text{s-Me}}$ = 148,021, **1**$_{\text{s-}i\text{-pro}}$ = 49,334, †**1**$_{\text{s-}tert\text{-Bu}}$ = 0; while relative absolute energies (kcal/mol) for **1**$_{\text{t-X}}$ series are **1**$_{\text{s-H}}$ = 197,401, **1**$_{\text{s-Me}}$ = 141,770, **1**$_{\text{s-}i\text{-pro}}$ = 49,345, ††**1**$_{\text{s-}tert\text{-Bu}}$ = 0 (†absolute energy = −427,553 kcal/mol; ††absolute energy = −427,508 kcal/mol).

(Tables 1–4). The B3LYP/6-31G** calculated order of $\Delta E_{\text{s-t,X}}$ between $\mathbf{3}_{\text{s-X}}$ and $\mathbf{3}_{\text{t-X}}$ is $\Delta E_{\text{s-t,Me}}$ (26.11 kcal/mol) > $\Delta E_{\text{s-t},i\text{-Pro}}$ (24.51 kcal/mol) ≈ $\Delta E_{\text{s-t},tert\text{-Bu}}$ (24.18 kcal/mol) ≈ $\Delta E_{\text{s-t,H}}$ (23.69 kcal/mol). This trend is precisely the same trend found earlier for structure $\mathbf{2}_{\text{X}}$. Hence, the same justifications can be applied.

Geometries, Dipole Moments, and Atomic Charges

The cyclic structures $\mathbf{1}_{\text{s-H}}$ and $\mathbf{1}_{\text{t-H}}$ have very similar geometrical parameters; both are planar with C_{2v} symmetry (Figs. 3 and 4). Substituting the hydrogen atoms by two methyl groups decreases symmetry to C_s; however, changes in geometrical parameters are negligible. When X is *i*-Pro, the changes are more considerable. The symmetries of $\mathbf{1}_{\text{s-}i\text{-Pro}}$ and $\mathbf{1}_{\text{t-}i\text{-Pro}}$ are C_s and C_1, respectively. ∠CSiC divalent angle in the cyclic $\mathbf{1}_{\text{t-}i\text{-Pro}}$ is larger than that of its corresponding $\mathbf{1}_{\text{s-}i\text{-Pro}}$. This is in contrary to the classic records of many acyclic carbenes and silylenes where the singlet divalent angle is smaller than the corresponding triplet divalent angle [4]. In triplet $\mathbf{1}_{\text{t-}i\text{-Pro}}$, the Si—C bond lengths are longer than those of their corresponding $\mathbf{1}_{\text{s-}i\text{-Pro}}$. Inversely, the C=C bond length in $\mathbf{1}_{\text{t-}i\text{-Pro}}$ is shorter than that of its corresponding $\mathbf{1}_{\text{s-}i\text{-Pro}}$. Fascinatingly, when X is *tert*-Bu, the cyclic structure **1** in singlet and triplet states is symmetric with C_{2v} point groups. Changes in geometrical parameters of $\mathbf{1}_{\text{s-}tert\text{-Bu}}$ and/or $\mathbf{1}_{\text{t-}tert\text{-Bu}}$ are as mentioned earlier for X is *i*-Pro. Every $\mathbf{2}_{\text{t-X}}$ species has higher (or equal) symmetries than their corresponding $\mathbf{2}_{\text{s-X}}$ (Fig. 4). The pronounced effect of substituting X in geometrical parameters of $\mathbf{2}_{\text{s-X}}$ and $\mathbf{2}_{\text{s-X}}$ is in the C=Si bond lengths. All $\mathbf{2}_{\text{t-X}}$ species have longer C=Si bond lengths than their corresponding $\mathbf{2}_{\text{s-X}}$. In acyclic structure **3**, stereochemical orientation of substituents X is in a way that torsion strain and steric hindrance diminish. Again, changes in geometrical parameters in structure **3** are considerable only for the C—Si bond lengths and the ∠XSiC divalent bond angles (Fig. 2). C—Si bond lengths of all $\mathbf{3}_{\text{s-X}}$ are longer than those of their corresponding $\mathbf{3}_{\text{t-X}}$. However, ∠XSiC divalent bond angles of all $\mathbf{3}_{\text{t-X}}$ are larger than those of their corresponding $\mathbf{3}_{\text{s-X}}$. This result is in contrast to that obtained earlier for cyclic structures **1**.

The trend of dipole moments for H_2C_2Si isomers is $\mathbf{2}_{\text{t-H}} > \mathbf{2}_{\text{s-H}} > \mathbf{1}_{\text{s-H}} > \mathbf{3}_{\text{s-H}} > \mathbf{1}_{\text{t-H}} > \mathbf{3}_{\text{t-H}}$ (Table 1). The trend of dipole moments for $(CH_3)_2C_2Si$ sets is $\mathbf{2}_{\text{s-Me}} > \mathbf{2}_{\text{t-Me}} > \mathbf{3}_{\text{s-Me}} > \mathbf{1}_{\text{t-Me}} > \mathbf{1}_{\text{s-Me}} > \mathbf{3}_{\text{t-Me}}$ (Table 2). The trend of dipole moments for $((CH_3)_2CH)_2C_2Si$ isomers is $\mathbf{1}_{\text{t-}i\text{-Pro}} > \mathbf{2}_{\text{t-}i\text{-Pro}} > \mathbf{2}_{\text{s-}i\text{-Pro}} > \mathbf{3}_{\text{s-}i\text{-Pr}} > \mathbf{1}_{\text{s-}i\text{-Pro}} > \mathbf{3}_{\text{t-}i\text{-Pro}}$ (Table 3). Finally, the trend of dipole moments for $((CH_3)_3C)_2C_2Si$ sets is $\mathbf{1}_{\text{t-}tert\text{-Bu}} > \mathbf{2}_{\text{t-}tert\text{-Bu}} > \mathbf{2}_{\text{s-}tert\text{-Bu}} > \mathbf{3}_{\text{s-}tert\text{-Bu}} > \mathbf{1}_{\text{s-}tert\text{-Bu}} > \mathbf{3}_{\text{t-}tert\text{-Bu}}$ (Table 4). These trends are contrary to those of previously reported for C_2H_2Si that all singlet states have larger dipole moments than their corresponding triplet states [3]. Fascinatingly, as the sizes of X become larger, the polarities of $\mathbf{1}_{\text{t-X}}$ increase. Moreover, the $\mathbf{2}_{\text{t-X}}$ species appear to have high polar structures.

The NBO method represents the electronic structure of a molecule in terms of the best possible resonance Lewis structure. The NBO analysis including atomic charges shows that in all 24 structures considered the divalentSi atoms have positive charges (Table 9). In contrast, C atoms directly attached to the Si atoms (C_2) have negative charges. Except for $\mathbf{2}_{\text{t-H}}$, in the rest of structures $\mathbf{3}_{\text{X}}$ and $\mathbf{2}_{\text{X}}$, C_3 atoms have rather high positive charges compared to the corresponding C_2 atoms. Interestingly, in $\mathbf{3}_{\text{s-X}}$ structures the magnitude of positive charges on the divalent Si atoms increases as the size of X increases: *tert*-Bu > *i*-pro > Me > H. Nevertheless, in the corresponding $\mathbf{1}_{\text{s-X}}$ and $\mathbf{2}_{\text{s-X}}$, the magnitude of positive charges on the divalent Si atoms is not sensitive to the employed substituents X (Table 9).

TABLE 9 NBO Analyses Including Atomic Charges of X_2-C_2Si Silylenes Confined to Three Structures **1–3**, Calculated at B3LYP/6-311++G** (where X is H, Me, *i*-pro, and *tert*-Bu)

		Atomic Charge				
Structure	*Species*	*Si*	*C_2*	*C_3*	*X_4*	*X_5*
1	$\mathbf{1}_{\text{s-H}}$	0.78	−0.63	−0.63	0.24	0.24
	$\mathbf{1}_{\text{t-H}}$	0.62	−0.55	−0.56	0.25	0.25
	$\mathbf{1}_{\text{s-Me}}$	0.77	−0.41	−0.41	−0.73	−0.73
	$\mathbf{1}_{\text{t-Me}}$	0.59	−0.34	−0.34	−0.74	−0.74
	$\mathbf{1}_{\text{s-}i\text{-pro}}$	0.76	−0.40	−0.40	−0.29	−0.29
	$\mathbf{1}_{\text{t-}i\text{-pro}}$	0.17	−0.23	−0.06	−0.31	−0.29
	$\mathbf{1}_{\text{s-}tert\text{-Bu}}$	0.75	−0.39	−0.39	−0.10	−0.10
	$\mathbf{1}_{\text{t-}tert\text{-Bu}}$	0.17	−0.15	−0.15	−0.10	−0.10
2	$\mathbf{2}_{\text{s-H}}$	0.71	−0.84	−0.32	0.23	0.23
	$\mathbf{2}_{\text{t-H}}$	0.50	−0.46	−0.56	0.26	0.26
	$\mathbf{2}_{\text{s-Me}}$	0.67	−0.87	0.11	−0.71	−0.71
	$\mathbf{2}_{\text{t-Me}}$	0.47	−0.47	−0.11	−0.69	−0.69
	$\mathbf{2}_{\text{s-}i\text{-pro}}$	0.67	−0.88	0.11	−0.27	−0.27
	$\mathbf{2}_{\text{t-}i\text{-pro}}$	0.46	−0.47	−0.11	−0.25	−0.25
	$\mathbf{2}_{\text{s-}tert\text{-Bu}}$	0.67	−0.87	0.12	−0.07	−0.07
	$\mathbf{2}_{\text{t-}tert\text{-Bu}}$	0.47	−0.47	−0.10	−0.05	−0.05
3	$\mathbf{3}_{\text{s-H}}$	0.77	−0.62	−0.14	−0.27	0.25
	$\mathbf{3}_{\text{t-H}}$	0.67	−0.62	−0.14	−0.16	0.25
	$\mathbf{3}_{\text{s-Me}}$	0.98	−0.62	0.07	−1.25	−0.76
	$\mathbf{3}_{\text{t-Me}}$	0.89	−0.63	0.07	−1.16	−0.76
	$\mathbf{3}_{\text{s-}i\text{-pro}}$	0.99	−0.61	0.07	−0.75	−0.33
	$\mathbf{3}_{\text{t-}i\text{-pro}}$	0.87	−0.62	0.06	−0.66	−0.32
	$\mathbf{3}_{\text{s-}tert\text{-Bu}}$	1.01	−0.62	0.07	−0.53	−0.12
	$\mathbf{3}_{\text{t-}tert\text{-Bu}}$	0.87	−0.62	0.06	−0.43	−0.12

CONCLUSION

In this paper, steric effects are found to affect the stability order of different isomeric X_2C_2Si sylilenes (where X is hydrogen (H), methyl (Me), isopropyl (*i*-pro), and *tert*-butyl (*tert*-Bu)). Relative energies are obtained through ab initio and DFT calculations at HF/6-31G*, B1LYP/6-31G*, B3LYP/6-31G*, MP2/6-31G*, HF/6-31G**, B1LYP/6-31G**, B3LYP/6-31G**, and MP2/6-31G** levels of theory. Among 24 silylenic structures considered, 7 structures are not real isomers. The order of stability for six structures of H_2C_2Si is $\mathbf{1}_{\text{s-H}}$ (0.00 kcal/mol) $>$ $\mathbf{2}_{\text{s-H}}$ (15.30 kcal/mol) $>$ $\mathbf{3}_{\text{s-H}}$ (20.85 kcal/mol) $>$ $\mathbf{2}_{\text{t-H}}$ (36.99 kcal/mol) $>$ $\mathbf{3}_{\text{t-H}}$ (44.54 kcal/mol) $>$ $\mathbf{1}_{\text{t-H}}$ (71.06 kcal/mol). Upon replacing hydrogen atoms by methyl groups, a new stability order obtained for $(CH_3)_2C_2Si$ is $\mathbf{1}_{\text{s-Me}}$ (0.00 kcal/mol) $>$ $\mathbf{3}_{\text{s-Me}}$ (13.84 kcal/mol) $>$ $\mathbf{2}_{\text{s-Me}}$ (18.98 kcal/mol) $>$ $\mathbf{3}_{\text{t-Me}}$ (39.95 kcal/mol) $>$ $\mathbf{2}_{\text{t-Me}}$ (44.74 kcal/mol) $>$ $\mathbf{1}_{\text{t-Me}}$ (68.45 kcal/mol). A nearly different order of stability found for (iso-propyl)$_2C_2Si$ isomers is $\mathbf{1}_{\text{s-}i\text{-pro}}$ (0.00 kcal/mol) $>$ $\mathbf{2}_{\text{s-}i\text{-pro}}$ (18.14 kcal/mol) $\approx$ $\mathbf{3}_{\text{s-}i\text{-pro}}$ (18.47 kcal/mol) $>$ $\mathbf{3}_{\text{t-}i\text{-pro}}$ (43.00 kcal/mol) $\approx$ $\mathbf{2}_{\text{t-}i\text{-pro}}$ (43.83 kcal/mol) $>$ $\mathbf{1}_{\text{t-}i\text{-pro}}$ (51.15 kcal/mol). Using the larger *tert*-butyl group, as a substituent (X), yet offers a more different stability order for six structures of (*tert*-butyl)$_2C_2Si$: $\mathbf{1}_{\text{s-}tert\text{-Bu}}$ (0.00 kcal/mol) $>$ $\mathbf{3}_{\text{s-}tert\text{-Bu}}$ (15.66 kcal/mol) $>$ $\mathbf{2}_{\text{s-}tert\text{-Bu}}$ (26.79 kcal/mol) $>$ $\mathbf{3}_{\text{t-}tert\text{-Bu}}$ (39.84 kcal/mol) $>$ $\mathbf{1}_{\text{t-}tert\text{-Bu}}$ (47.46 kcal/mol) $>$ $\mathbf{2}_{\text{t-}tert\text{-Bu}}$ (49.28 kcal/mol). Linear correlations are found between the LUMO–HOMO energy gaps of the singlet $\mathbf{1}_{\text{s-X}}$ and $\mathbf{2}_{\text{s-X}}$, and their corresponding singlet–triplet energy separations calculated at B3LYP/6-31G** level. The highest dipole moment is found for $\mathbf{1}_{\text{t-}tert\text{-Bu}}$; however, the lowest dipole moment is found for $\mathbf{3}_{\text{t-H}}$. Among all the calculation methods employed, B3LYP is the method of choice.

ACKNOWLEDGMENTS

We gratefully thank A. Ghaderi of Chemistry Department, Imam Hossein University for his useful discussion and suggestions. We also acknowledge the cordial collaboration with Dr. Y. Fathollahi as well as with S. Souri, F. Buazar, N. Jalalimanesh, and M. Ghavami (Chemistry Department of Tarbiat Modares University).

REFERENCES

[1] Ishikawa, M.; Kumada, M. Adv Organomet Chem 1981, 19, 51.

[2] Riviere, P.; Castel, A. J. Satgt, J Am Chem Soc 1980, 102, 5413.

[3] Kassaee, M. Z.; Musavi, S. M.; Buazar, F.; Ghambarian, M. J Mol Struct (Theochem) 2005, 722, 151.

[4] Gaspar, P. P.; West, R.; In The Chemistry of Organic Silicon Compounds; Rappoport, Z.; Apeloig, Y. (Eds.); Wiley: New York, 1998; Vol. 2, part 3, Ch. 43.

[5] Kassaee, M. Z.; Ghambarian, M.; Musavi, S. M. J Organomet Chem 2005, 690, 4692.

[6] Olbrich, G. Chem Phys Lett 1980, 73, 110.

[7] Saxe, P.; Schaefer, H. F., III; Handy, N. J Phys Chem 1981, 85, 745.

[8] Kalcher, J.; Sax, A. F. J Mol Struct (Theochem) 1992, 253, 287.

[9] Reisenauer, H. P.; Maier, G.; Reimann, A.; Hoffmann, R. W. Angew Chem, Int Ed 1984, 96, 596.

[10] Redondo, J. R.; Redondo, P.; Largo, A. J Mol Struct (Theochem) 2003, 621, 59.

[11] Ando, W.; Fujita, M.; Yoshida, H.; Sekiguchi, A. J Am Chem Soc 1988, 110, 3310.

[12] Pae, D. H.; Xiao, M.; Chiang, M. Y.; Gaspar, P. P. J Am Chem Soc 1991, 113, 1281.

[13] Weidenbruch, M.; SchPfer, A.; Peters, K.; Von Schnering, H. G. J Organomet Chem 1986, 314, 25.

[14] Weidenbruch, M.; Brand-Roth, B.; Pohl, S.; Saak, W. Angew Chem, Int Ed Engl 1990, 29, 90.

[15] Denk, M.; Hayashi, R. K.; West, R. J Chem Soc, Chem Commun 1994, 33.

[16] Pitzer, K. S. J Am Chem Soc 1948, 70, 2140.

[17] Mulliken, R. S. J Am Chem Soc 1950, 72, 4493.

[18] Okazaki, R.; Tokitoh, N.; Matsumoto, T. In Synthetic Methods of Organometallic and Inorganic Chemistry; Herrmann, W. A. (Ed.); Thieme: New York, 1996; Vol. 2, p. 260.

[19] Goldberg, D. E.; Harris, D. H.; Lappert, M. F.; Thomas, K. M. J Chem Soc, Chem Commun 1976, 261.

[20] West, R.; Fink, M. J.; Michl, J. Science 1981, 214, 1343.

[21] Masamune, S.; Hanzawa, Y.; Murakami, S.; Bally, T.; Blount, J. F. J Am Chem Soc 1982, 104, 1150.

[22] Masamune, S.; Hanzawa, Y.; Williams, D. J. J Am Chem Soc 1982, 104, 6163.

[23] Masamune, S.; Sita, L. R. J Am Chem Soc 1985, 107, 6390.

[24] Weidenbruch, M. Organometallics 2003, 22, 4348.

[25] Ishida, S.; Iwamoto, T.; Kabuto, C.; Kira, M. Nature 2003, 421, 725.

[26] Wiberg, N.; Lerner, H. W.; Vasisht, S. K.; Wagner, S.; Karaghiosoff, K.; Noth, H.; Ponikwar, W. Eur J Inorg Chem 1999, 1211.

[27] Maier, G.; Reisenauer, H. P.; Egenolf, H.; Glatthaar, J. Eur J Org Chem 1998, 1307.

[28] Maier, G.; Pacl, H.; Glatthaar, J.; Reisenauer, H. P.; Meudt, A.; Janoschek, R. J Am Chem Soc 1994, 117, 12712.

[29] Popelier, P. L. A. Comput Phys Commun 1996, 93, 212.

[30] Becke, A. D. J Chem Phys 1996, 104, 1040.

[31] Adamo C.; Barone, V. Chem Phys Lett 1997, 274, 242.

[32] Saebo, S. Almlof, J. Chem Phys Lett 1989, 154, 83.

[33] Carpenter, J. E.; Weinhold, F. J Mol Struct (Theochem) 1988, 41, 169.

[34] Hout, R. F.; Levi, B. A.; Heher, W. J. J Comput Chem 1985, 82, 234.

[35] Defrees, D. J.; McLean, A. D. J Chem Phys 1985, 82, 333.

[36] Frisch, M. J.; Trucks, G. W.; Schlegel, H. B.; Scuseria, G. E.; Robb, M. A.; Cheeseman, J. R.; Zakrzewski, V. G., Jr.; Montgomery, J. A.; Stratmann, R. E.; Burant, J. C.; Dapprich, S.; Millan, J. M.; Daniels, A. D.; Kudin, K. N.; Strain, M. C.; Farkas, O.; Tomasi, J.; Barone, V.; Cossi, M.; Cammi, R.; Mennucci, B.; Pomelly, C.; Adamo, C.; Clifford, S.; Ochterski, J.; Petersson, G. A.; Ayala, P. Y.; Cui, Q.; Morokuma, K.; Malick, D. K.; Rabuck, A. D.; Raghavachari, K.; Foresman, J. B.; Cioslowski, J.; Ortiz, J. V.; Baboul, A. G.; Stefanov, B. B.; Liu, G.; Liashenko, A.; Piskorz, P.; Komaromi, I.; Gomperts, R.; Martin, R. L.; Fox, D. J.; Keith, T.; Al-Laham, M.A.; Peng, C. Y.; Nanayakkara, A.; Gonzalez, C.; Challacombe, M.; Gill, P. M. W.; Johnson, B.; Chen, W.; Wong, M. W.; Andres, J. L.; Gonzalez, C.; Head-Gordon, M.; Replogle, E. S.; Pople, J. A. 98, Gaussian Inc., Pittsburgh, PA, 1998.

[37] Barrientos, C.; Redondo, P.; Largo, A. J Phys Chem A 2000, 104, 11541.

[38] Barrientos, C.; Cimas, A.; Largo, A. J Phys Chem A 2001, 105, 6724.

[39] Kassaee, M. Z.; Musavi, S. M.; Hamadi, H.; Ghambarian, M.; Hosseini, S. E. J Mol Struct (Theochem) 2005, 730, 33.

[40] Kassaee, M. Z.; Musavi, S. M.; Ghambarian, M. J Mol Struct (Theochem) 2005, 731, 225.

[41] Wong, M. W.; Radom, L. J Am Chem Soc 1993, 115, 1507.

[42] Kassaee, M. Z.; Hossaini, Z.; Haerizade, B. N.; Sayyed-Alangi, S. Z. J Mol Struct (Theochem) 2004, 676, 129.